PML recruits TET2 to regulate DNA modification and cell proliferation in response to chemotherapeutic agent

Chengli Song[#,1], **Lina Wang**[#,1], **Xiaoyan Wu**[1], **Kai Wang**[1], **Dan Xie**[1], **Qi Xiao**[1], **Songyu Li**[1], **Kui Jiang**[1], **Lujian Liao**[2], **John R. Yates III**[3], **Jiing-Dwan Lee**[4], and **Qingkai Yang**[1]

[1] Department of Oncology, Second Affiliated Hospital, Institute of Cancer Stem Cell, DaLian Medical University, 9 Western Lvshun South Road, Dalian, Liaoning 116044, China.

[2] Shanghai Key Laboratory of Regulatory Biology, School of Life Sciences, East China Normal University, Shanghai, 200241, China.

[3] Department of Chemical Physiology, The Scripps Research Institute, 10550 North Torrey Pines Road, La Jolla, CA 92037, USA.

[4] Department of Immunology and Microbial Science, The Scripps Research Institute, 10550 North Torrey Pines Road, La Jolla, CA 92037, USA.

[#] These authors contributed equally to this work.

Abstract

Aberrant DNA methylation plays a critical role in the development and the progression of cancer. Failure to demethylate and to consequently reactivate methylation-silenced genes in cancer contributes to chemotherapeutic resistance, yet the regulatory mechanisms of DNA demethylation in response to chemotherapeutic agents remain unclear. Here, we show that promyelocytic leukemia (PML) recruits ten-eleven translocation dioxygenase 2 (TET2) to regulate DNA modification and cell proliferation in response to chemotherapeutic agents. TET2 was required by multiple chemotherapeutic agents (such as doxorubicin) to promote 5-hydroxymethylcytosine (5hmC) formation. Stable isotope labeling with amino acids in cell culture, followed by immunoprecipitation-mass spectrometry, identified potential binding partners of TET2, of which PML mostly enhanced 5hmC formation. PML physically bound to TET2 via the PML C-terminal domain and recruited TET2 to PML-positive nuclear bodies. This interaction was disrupted by the PML-RARA t(15;17) mutation, which stems from chromosomal translocation between DNA encoding the C-terminal domain of PML and the retinoic acid receptor alpha (RARA) gene. In response to chemotherapeutic drugs, PML recruited TET2, regulated DNA modification, reactivated methylation-silenced genes, and impaired cell proliferation. Knockout of PML abolished doxorubicin-promoted DNA modification. In addition, PML and TET2 levels positively correlated with improved overall survival in patients with head and neck cancer. These findings

Corresponding Author: Qingkai Yang, Department of Oncology, Second Affiliated Hospital, Institute of Cancer Stem Cell, DaLian Medical University, 9 Western Lvshun South Road, Dalian, Liaoning 116044, China. Phone: 86-0411-86118631; Yangqingkai@dmu.edu.cn.

shed insight into the regulatory mechanisms of DNA modification in response to chemotherapeutic agents.

Keywords

Ten-eleven translocation dioxygenase; 5-hydroxymethylcytosine; Promyelocytic leukemia

Introduction

Abnormal DNA methylation is a hallmark of cancer (1, 2). Aberrant DNA methylation of multiple genes results in their inappropriate transcriptional silencing and contributes to loss of checkpoints and other functions in cancer. In response to therapy, failure to demethylate and to consequently reactivate these methylation-silenced genes contributes to therapeutic resistance (2). This is at least in part because the activity of most therapies depends to some extent on the same apoptotic/proapoptotic and differentiation/prodifferentiation pathways, which are silenced by DNA methylation during carcinogenesis (2), and one of the highly possible reasons for the failure to demethylate these genes is the deregulation of ten-eleven translocation (TET).

TET family members (TET1, TET2, and TET3) oxidate 5-methylcytosine (5mC) to 5-hydroxymethylcytosine (5hmC) and consequently promote DNA demethylation (3). Accumulating studies indicate that TETs play critical roles in various physical and pathological processes, including tumorigenesis, cell reprogramming, development, and differentiation (4–6). Compared with TET1 and TET3, TET2 shows much higher mutant frequencies in multiple types of cancer. TET2 is often mutated in glioma, lymphoid, and myeloid malignancies, especially acute myeloid leukemia (AML) (7–9). In AML patients, TET2 mutations are associated with reduced response of AML to chemotherapy and adverse overall survival (10, 11). Interestingly, TET2 mutations have been reported to be mutually exclusive with isocitrate dehydrogenase 1/2 (IDH1/2) (12, 13) and Wilms' tumor (WT1) mutations (14, 15). Both IDH1/2 and WT1 mutations lead to reduced TET2 activity and reductions in 5hmC (12–15). Furthermore, the decrease of TETs and 5hmC was identified as a hallmark of multiple types of solid tumor (16, 17) and, importantly, enhanced expression of TET2 suppresses both proliferation and metastasis of cancer cells (16, 18).

Like TET2, promyelocytic leukemia (PML) is also frequently mutated in AML (19). PML plays a critical role in cell-cycle arrest, senescence, apoptosis, genome stability, and antiviral effects (20). The t(15;17) mutation of PML and retinoic acid receptor alpha (RARA) results in PML-RARA fusion protein and leads to acute promyelocytic leukemia (APL). Unlike PML, PML-RARA interacts with DNA methyltransferase 3s (DNMT3), promotes DNA methylation of tumor suppressors, and leads to transcription repression (19, 21), which is essential for PML-RARA to initiate APL (22). Arsenic acid (As_2O_3) and/or all-trans retinoic acid (RA) dissociate repressor complexes from PML-RARA, mediate PML-RARA subsequent degradation, and effectively induce differentiation or apoptosis of AML cells (19). Except RA and As_2O_3, PML also responds dynamically to many chemotherapeutic agents (such as doxorubicin) to form PML-nuclear bodies (PML-NB), which recruit

numerous proteins (such as p53 and RB1) to facilitate the inhibition of cancer (20, 23). In this study, we show that PML recruits TET2, regulating DNA modification and cell proliferation in response to chemotherapeutic agents (Fig. 1A).

Materials and Methods

Cell culture and transfection

HEK293 (human embryonic kidney), SCC-15 (human head and neck squamous cell carcinoma), SCC-25 (human head and neck squamous cell carcinoma), and U2OS (human osteosarcoma) cells from the ATCC were maintained in DMEM containing 10% heat-inactivated FBS, 2 mM glutamine, 100 U/mL penicillin, and streptomycin at 37°C under a humidified atmosphere of 5% CO_2. $Pml^{+/+}$ and $Pml^{-/-}$ mouse embryonic fibroblast (MEF) cells were previously described (24). NB4 (acute promyelocytic leukemia) cells from Shanghai Institute of Hematology, Ruijin Hospital (Shanghai, China), were cultured in suspension under standard conditions. Mycoplasma PCR testing of these cells was performed every month. Transfections were performed using Lipofectamine 2000 (Thermo Fisher Scientific Inc.).

SILAC-labeling and mass spectrometry analysis

Stable isotope labeling by amino acids in cell culture (SILAC)-labeling and mass spectrometry (MS) analysis were performed as previously described (24–26). Briefly, the light-labeled HEK293 cells were transfected with pCI-Neo HA-TET2 for 36 hrs, while heavy-labeled ([U-$^{13}C_6$]-L-lysine and [U-$^{13}C_6$, $^{15}N_4$]-L-arginine) cells were transfected with pCI-Neo. "Light" cell lysate and "heavy" lysate were mixed at a 1:1 ratio, and the mixed lysates were incubated with the anti-HA antibody for 4 hrs, followed by MS analysis.

Plasmids, cell lines, and antibodies

pAd Track-CMV (pAd-EV) and pAd-PML (flag tagged PML IV) were described in a previous study (24). pCI-Neo Flag-PML isoforms, HA-PML, pCDNA3B Flag-TET2, and catalytic dead mutant pCDNA3B Flag-TET2 MUT (H1304Y, D1306A) plasmids were described in our previous studies (27, 28). pS-Flag-SBP TET2 and TET2 deletion mutants (Flag-TET2) were generous gifts from Dr. Yu at University of Michigan Medical School (Ann Arbor, MI; ref. 29). Full-length TET2 sequence from pS-Flag-SBP TET2 was cloned into the E*co*R I and S*al* I sites of the vector pEGFP C1 (BD Biosciences) to build pEGFP TET2 plasmid. Similarly, full-length TET2 sequence from pS-Flag-SBP TET2 was cloned into the S*al* I and N*ot* I sites of the vector pCI-Neo (Promega) to build pCI-Neo Flag-TET2 and pCI-Neo HA-TET2 plasmids. pEGFP DNMT3A, pEGFP DNMT3B, and pcDNA3.1 PML-RARA were kind gifts from Dr. Robertson (30) and Dr. Ley (31), respectively. PML-RARA sequence from pcDNA3.1 PML-RARA was cloned into the E*co*R I and X*ba* I sites of pCI-Neo to build pCI-Neo Flag-PML-RARA. Sim2 amplified from MEF cDNA was cloned into the X*ba* I and N*ot* I sites of lentivector pCDH (System Biosciences) to build pCDH Flag-Sim2. Sequences of shTETs and shPML described in Supplementary Table S1 were used to build pLKO.1 shPML#1/#2, pLKO.1 shTET1#1/#2, pLKO.1 shTET2#1/#2, and shTET3#1/#2 plasmids. Sequences of shPML#1 and shPML#2 were also cloned into pMKO.1-hyg to build pMKO.1 shPML#1 and pMKO.1 shPML#2. The pLX304 library

containing 65 potential functional partners of TET2 was from GE Healthcare. Pml knockout and WT MEF cell lines were generous gifts from Dr. Myung Kim at the NIH (Bethesda, MD) and Dr. Giovanni Blandino at the Regina Elena Cancer Institute, Rome, Italy. Recombinant adenoviral, lentiviral, and retroviral particles were generated according to the standard protocols. Antibodies are described in Supplementary Table S1.

LC/MS MS analysis of C, 5mC, and 5hmC

LC/MS MS analyses of C, 5mC, and 5hmC were carried out as previously described (28).

Immunoblotting, immunofluorescence, and immunoprecipitation

Immunoblotting, immunofluorescence, and immunoprecipitation were carried out as previously described (24).

siRNA knockdown

siRNA knockdown was carried out as previously described (24, 32). Briefly, siRNAi against Tet1, Tet2, Tet3, or Sim2 was performed using siGenome SMART pool siRNA reagents (Dharmacon). Nontargeting siRNA (Dharmacon) was used as control.

5hmC dot blot assay

Different doses of genomic DNA were spotted on Hybond-N+ membrane, then spotted DNA was cross-linked to the membrane by UV Stratalinker 2400 (Stratagene), then membrane was blocked in 5% BSA and subsequently incubated with anti-5hmC antibody.

Cell synchronization

L-mimosine (G1), thymidine (S), and nocodazole (G2/M) were used to synchronize cells as previously described (33).

qRT-PCR

RNA was extracted using the miRNeasy Mini Kit (QIAGEN). Reverse transcription was carried out using the PrimeScript RT Reagent Kit (TaKaRa). qRT-PCR was performed with the SYBR PrimeScript PCR kit II (TaKaRa). Primers for qRT-PCR are described in Supplementary Table S1.

Generation of stable cell lines

To generate stable TET1, TET2, TET3, and PML knockdown cells, HEK293, SCC-15, and SCC-25 cells were infected with virus encoding pLKO.1 scrambled shRNA, pLKO.1 shPML#1/#2, pLKO.1 shTET1#1/#2, pLKO.1 shTET2#1/#2, or pLKO.1 shTET3#1/#2 to build stable knockdown cells. Cells were selected with 1 μg/mL puromycin for 2 weeks, then pLKO.1 shTET2#1 and pLKO.1 shTET2#2 stable cells were infected with the virus encoding pMKO.1 shPML#1 or pMKO.1 shPML#2. Resultant cells were selected in 200 μg/mL hygromycin B for 2 weeks to generate stable PML+TET2 double knockdown cells.

Whole-genome bisulfite-sequencing

$Pml^{+/+}$ and $Pml^{-/-}$ MEF cells were treated with mock or doxorubicin for 24 hrs. The genomic DNA was extracted and purified from samples using Qiagen DNeasy Kit (QIAGEN). After DNA-end repair and 3'-dA overhung, the 100–200 bp fragments were converted with ZYMO EZ DNA Methylation-Gold Kit (Zymo Research) according to manufacturer's instruction. Then the bisulphite- converted DNA samples ($Pml^{+/+}$ Ctrl, $Pml^{+/+}$ Dox, $Pml^{-/-}$ Ctrl, and $Pml^{-/-}$ Dox) were sequenced by Illumina HiSeq 2000 using Illumina standard protocol. Resultant reads were mapped onto the mouse genome reference sequence (Jul. 2007, mm9) using the alignment software 'segemehl' version 0.1.7 (www.bioinf.uni-leipzig.de). Only reads uniquely aligned to the mm9 assembly of the mouse genome were retained. Only the methylation sites with the number of reads 10 were used for further analysis. Methylation rate of sites was calculated using the formula: methylation rate (MR) = rC/(rC + rT), where rC is the number of reads that remain C after bisulfite treatment (methylated reads), and rT is the number of reads that become T after bisulfite treatment (unmethylated reads). Chi-square test was used to calculate the P value of the methylation difference between control (Mock) and doxorubicin (Dox) treatment. Methylation sites with $P < 0.05$ and absolute methylation difference 50% were considered significant. To identify candidate differentially methylated regions (DMR) between Dox and Mock, their peaks were merged, and the number of reads within those peaks was assessed with chi-square test. DMRs with MR (Dox)/MR (Mock) < 0.4 and $P < 0.05$ (chi-square test) were classified as doxorubicin-promoted demethylation regions (DPD-DMR). The genes with DPD-DMRs located in ± 10 KB of transcription start sites (TSS) were used for further study. All sequencing data were deposited to the NCBI under the accession number GSE75408.

hMEDIP-qPCR

5-hydroxymethylcytosine methylated DNA immunoprecipitation (hMEDIP) was carried out as previously described (34, 35).

Statistical analysis

P values were calculated using Student t test or chi-square test as noted. $P < 0.05$ was considered statistically significant (*).

MTT assay

3-(4,5)-Dimethylthiahiazo(-z-y1)-3,5-di-phenytetrazoliumromide (MTT) assay was carried out as previously described (24).

Xenografts

The following animal handling procedures were approved by the Animal Care and Use Committee of DaLian Medical University. Xenograft models were carried out as previously described (24). Briefly, 1 X 10^7 cultured SCC-15 cells stably expressing shScram (control scrambled shRNA), shPML (shPML#1), shTET2 (shTET2#1), or shPML/shTET2 (shPML#1/shTET2#1) were suspended in DMEM and injected subcutaneously into the flank of 6-week-old Nod/Scid mice. After 12 days, these tumor-bearing mice were

randomized into 8 groups (6 mice per group) and injected i.p. every 3 days with vehicle or doxorubicin (3 mg/kg). After 21 days, the mice with vehicle treatment were sacrificed. Tumor size was measured every 3 days by caliper and tumor volumes were calculated using the formula $0.52 \times L \times W^2$, where L was the longest diameter and W was the shortest diameter.

Results

TET2 promotes DNA 5hmC modification in response to chemotherapeutic agents

Considering that the DNA modification pathway might be deregulated in cancer cells, we first used MEF cells (normal cells) to determine the alteration of DNA modification in response to chemotherapeutic agents. The DNA 5mC and 5hmC levels of the treated MEF cells were assessed by MS as described in our previous study (28). The nucleosides were quantified using the nucleoside to base ion mass transitions of 228 to 112 (C), 242 to 126 (5mC) and 258 to 142 (5hmC) (Fig. 1B). MS analyses indicated that the 5hmC level (5hmC/C) was increased about 1.5-fold by doxorubicin treatment (Fig. 1C), whereas 5mC level (5mC/C) was not notably altered by doxorubicin (Supplementary Fig. S1A). Further dot blotting also indicated that 5hmC was increased by doxorubicin (Fig. 1D). To determine whether the increase of 5hmC is a phenomenon simply related to cell-cycle or cell growth arrest, MEF cells were treated with L-mimosine, thymidine, or nocodazole to induce G1, S, or G2/M distribution (Supplementary Fig. S1B). MS analyses demonstrated that synchronized MEF cells showed less than 10% alteration of 5mC (Supplementary Fig. S1C) and 5hmC (Supplementary Fig. S1D). Therefore, it was unlikely that doxorubicin-promoted increase of 5hmC was stemmed from cell-cycle arrest. Due to low oxygen concentration decreases in the *in vivo* activity of oxygen-dependent TETs (36), we supposed that TETs might play more notable roles in head and neck squamous cell carcinoma (HNSC), which is likely exposed to more oxygen. Therefore, HNSC SCC-15 and SCC-25 cells were used for further study. HEK293 cells frequently showing high transfection rate (over 90%) were also used. To determine whether doxorubicin can promote 5hmC in other cell lines, we then treated HEK293, SCC-15, and SCC-25 cells with doxorubicin. MS analyses demonstrated that doxorubicin enhanced 5hmC in these cell lines (Fig. 1E). Next, we examined whether 5hmC was increased by other chemotherapeutic agents, such as mitomycin C and cisplatin. As shown in Fig. 1F, 5hmC was also increased by mitomycin C and cisplatin in multiple cell lines, whereas 5mC was not altered by doxorubicin, mitomycin C, or cisplatin (Supplementary Fig. S1E and S1F).

To identify which TET is responsible for chemotherapy-promoted 5hmC, we first examined the alteration of protein and expression levels of TETs in response to doxorubicin. As shown in Fig. 1G, the protein levels of Tet1, Tet2, or Tet3 were not altered by doxorubicin in MEF cells. Further qRT-PCR also demonstrated that the expression of Tet1, Tet2, or Tet3 was not notably altered by doxorubicin (Supplementary Fig. S1G). In line with the results of MEF cells, the expression of TET1, TET2, or TET3 was not notably altered by doxorubicin in HEK293, SCC-15, and SCC-25 cells (Supplementary Fig. S1H). It seemed that doxorubicin-promoted 5hmC was not stemmed from the alteration of TET protein or expression level. We then performed knockdown of TET by RNAi/shRNAi to identify which TET is

responsible for chemotherapy-promoted 5hmC. MEF cells were treated with siRNAs against Tet1, Tet2, or Tet3. The knockdown efficiency of TETs was determined by Western blotting (Supplementary Fig. S1I) and qRT-PCR (Supplementary Fig. S1J). As shown in Fig. 1H, knockdown of Tet2 notably diminished doxorubicin-promoted 5hmC. To further evaluate the impact of TET2 on doxorubicin-promoted 5hmC in other cell lines, we created HEK293, SCC-15, and SCC-25 cells stably expressing scramble shRNA (control), shmTET1 (#1/#2), shmTET2 (#1/#2), or shmTET3 (#1/#2). The knockdown efficiencies were validated by qRT-PCR (Supplementary Fig. S1K–S1M). Consistent with the observation in MEF cells, doxorubicin-promoted 5hmC in HEK293 (Fig. 1I), SCC-15 (Fig. 1J), and SCC-25 (Fig. 1K) cells was also decreased by the knockdown of TET2 (Fig. 1I-1K). Hence, it seemed that TET2 promotes DNA 5hmC modification in response to doxorubicin.

PML physically binds to TET2 and recruits TET2 to PML nuclear bodies

To identify the candidate functional partners of TET2 in response to chemotherapy, SILAC MS analysis of anti-TET2 coimmunoprecipitation (co-IP) was carried out (Fig. 2A). SILAC MS analyses identified 492 peptides with over 1×10^6 peak area (Supplementary Table S2). Sixty-five proteins with at least two peptides were considered as the potential partners of TET2. KEGG pathway analysis indicated that the 65 genes were enriched in "immune response," "RNA degradation," and "hypoxia" pathways (Supplementary Fig. S2A). In line with the previous study (29), *O*-linked *N*-acetylglucosamine transferase was also identified to interact with TET2 (Supplementary Table S2).

Next, we investigated the role of 65 genes in the regulation of the TET2 catalytic product, 5hmC. Plasmids encoding 65 genes were transfected into HEK293. MS analyses of the resultant cells demonstrated that PML showed the most notable ability to enhance 5hmC (Fig. 2B), while none of the 65 genes notably altered the 5mC levels (Supplementary Fig. S2B). Due to the critical roles of PML in chemo-response and its most notable ability to increase 5hmC, we reasoned that PML was a functional partner of TET2.

Considering that PML is well known to form the PML-NBs and to recruit proteins to regulate transcription, we then determined whether PML could recruit TET2 to PML-NBs. The ability of endogenous PML-TET2 association in HEK293 cells was first assessed by co-IP (Fig. 2C). Western blotting of the resultant immunoprecipitates indicated that the endogenous PML-TET2 association was detected. As mentioned above, unlike PML-RARA, PML shows poor interaction and colocalization with DNMT3s (19, 21). Therefore, TET2 and PML (isoform IV) were overexpressed in HEK293, using DNMT3A and DNMT3B as controls. Consistent with the observation of endogenous PML and TET2, co-IP analyses indicated that overexpressed PML showed more notable interaction with overexpressed TET2 than with overexpressed DNMT3A (Fig. 2D). Furthermore, TET2, PML, and DNMT3 were overexpressed in U2OS cells, which are often used for immunofluorescent analysis. Immunofluorescent analysis demonstrated that overexpressed TET2, DNMT3A, and DNMT3B were nuclear diffuse in the absence of overexpressed PML (Fig. 2E and 2F), whereas only overexpressed TET2 was delocalized to PML-NBs in U2OS cells overexpressing PML (Fig. 2G and 2H). Hence, compared with DNMT3s, TET2 and PML preferably bound to each other.

PML-RARA t(15;17) mutation disrupts the ability of PML to bind to TET2

To determine the regions of TET2 that bind to PML, HEK293 cells were transfected with plasmids encoding PML and each of the TET2-deletion mutants (Fig. 3A). Co-IP analyses of the resultant cells demonstrated that overexpressed TET2-F2 (Cys-rich domain) showed poor interaction with overexpressed PML, whereas TET2-F1, TET2-F3, and TET2-F4 showed notable interaction with PML (Fig. 3B). Then we extended our analysis of the interaction between overexpressed PML and each of the TET2-deletion mutants in U2OS cells by immunofluorescence. Without the transfection of PML, TET2-deletion mutants were nuclear or cytoplasm diffuse (Fig. 3C and 3D). With the transfection of PML, only TET2-F2 (Cys-rich domain) was not delocalized to the PML-NBs, whereas TET2-F1, TET2-F3, and TET2-F4 were colocalized with PML-NBs (Fig. 3E and 3F).

To determine the regions of PML to interact with TET2, HEK293 and U2OS cells were transfected with the plasmids encoding TET2 and each of the nuclear-located PML isoforms (PML I-VI) (Fig. 4A). PML isoforms are generated from a single PML gene by alternative splicing (37). These PML isoforms share the same N-terminal region but differ in their C-terminal sequences (Fig. 4A). Co-IP analyses of HEK293 cells transfected with TET2 and each of the PML isoforms indicated that TET2 could bind all PML isoforms except PML V (Fig. 4B). Among PML isoforms, PML IV showed the most notable ability to bind to TET2. Consistent with the result of co-IP, immunofluorescent analyses of U2OS cells also demonstrated that TET2 showed poor colocalization with PML V. Among PML isoforms, TET2 preferably, but not exclusively, bound PML IV (Fig. 4C). Because PML isoforms share the same N-terminal, these observations suggested that PML bound to TET2 in a PML C-terminal-dependent way.

Considering that PML-RARA results from the displacement of PML C-terminal with RARA, we then evaluated the ability of PML-RARA to bind TET2 to confirm that the binding between PML and TET2 is dependent on PML C-terminal. We first carried out co-IP analysis to assess the interaction between TET2 and PML-RARA. DNMT3A, which was reported to interact with PML-RARA (19, 21), was used as control. We found that DNMT3A notably bound PML-RARA, whereas TET2 poorly bound PML-RARA (Fig. 4D). Next, we evaluated the impact of PML-RARA mutation on the DNA modification. Using pCI-NEO vector as control, we overexpressed PML or PML-RARA in HEK293 cells. Dot blotting demonstrated that PML-RARA mutation disrupted the ability of PML to enhance 5hmC (Fig. 4E). Further MS analyses confirmed that PML-RARA mutation diminished the PML-enhanced 5hmC (Fig. 4F) without significant alteration of 5mC (Supplementary Fig. S3A). We then investigated the impact of endogenous PML restoration on 5hmC in APL cells, which harbor an endogenous PML-RARA mutation. To restore the function of PML, As_2O_3 and RA were used to treat NB4 cells (APL cells) (19). Without significant alteration of 5mC (Supplementary Fig. S3B), As_2O_3 or RA promoted endogenous PML-RARA degradation and restored endogenous PML ability to enhance 5hmC (Fig. 4G and 4H). Finally, we investigated the mutual exclusivity between PML-RARA and TET2 mutations in AML. A meta-analysis of 2054 AML cases was carried out (38–41). The frequently AML-mutant genes IDH1, IDH2, WT1, DNMT3A, RUNX1 (runt-related transcription factor 1), and FLT3 (fms-related tyrosine kinase 3) were taken as controls. As shown in Fig. 4I and

Supplementary Fig. S3C-S3E, PML-RARA showed a mutually exclusive pattern with TET2 mutations in AML (odds ratio: 0.069; $P < 0.001$), whereas PML-RARA or TET2 mutations showed no mutually exclusive pattern with FLT3 mutations.

PML recruits TET2 to regulate 5hmC in response to doxorubicin

To investigate the role of PML in regulation of TET2 in response to chemotherapy, we first investigated the alteration of endogenous PML and TET2 localization by doxorubicin treatment. As shown in Fig. 5A, Supplementary Fig. S4A and S4B, both endogenous TET2 and endogenous PML were nuclear diffuse in the cells without doxorubicin treatment, while doxorubicin promoted the formation of PML-NB and the recruitment of TET2 to PML-NBs. As described above, doxorubicin treatment increased Pml protein level (Fig. 5B) and 5hmC (Fig. 1C-1E), and no notable alteration of Tet1, Tet2, or Tet3 was detected (Fig. 1G and Supplementary Fig. S4C), suggesting that doxorubicin-promoted 5hmC was not stemmed from the alteration of TET protein levels. In addition, PML is well known to form PML-NBs and to recruit numerous proteins to PML-NBs in response to chemotherapy. Therefore, we reasoned that PML recruits TET2 to regulate 5hmC in response to chemotherapeutic agent.

Then we evaluated the role of endogenous PML in chemotherapy-promoted 5hmC using $Pml^{+/+}$ (wild type, WT) and $Pml^{-/-}$ (knockout, KO) MEF cells. Dot blotting and MS analyses indicated that knockout of Pml diminished the doxorubicin-promoted 5hmC (Fig. 5B and 5C) without significant alteration of genomic-scale 5mC (Supplementary Fig. S4D). Importantly, the adenovirus-mediated expression of PML restored the ability of doxorubicin to promote 5hmC in $Pml^{-/-}$ cells (Fig. 5D and 5E) without significant alteration of 5mC (Supplementary Fig. S4E), which suggested that PML was essential for TET2-promoted 5hmC in response to chemotherapy. Next, we evaluated the effect of Pml and/or Tet2 knockout on doxorubicin-promoted 5hmC. We found that doxorubicin-promoted 5hmC was decreased by the depletion of either Tet2 or Pml gene, but not additively by the codepletion of both genes (Fig. 5F). To further investigate the impact of PML-TET2 on doxorubicin-promoted 5hmC in other cell lines, we created HEK293, SCC-15, and SCC-25 cells stably expressing scramble shRNA (control), shmTET2 (#1 and #2), and/or shmPML (#1 and #2). The knockdown efficiencies were validated by qRT-PCR (Supplementary Fig. S4F–S4H). Consistent with the observation in MEF cells, doxorubicin-promoted 5hmC in HEK293 (Fig. 5G), SCC-15 (Fig. 5H), and SCC-25 (Fig. 5I) cells was also decreased by the depletion of either TET2 or PML, but not additively by the codepletion of both genes (Fig. 5G-5I).

Knockout of PML diminishes doxorubicin-promoted demethylation

Considering that 5hmC is supposed to be the intermediate of DNA demethylation, we carried out whole genomic bisulfite sequencing to evaluate the role of PML in doxorubicin-promoted DNA demethylation (Fig. 6A). Briefly, $Pml^{+/+}$ and $Pml^{-/-}$ MEF cells were treated with doxorubicin for 24 hrs, then the bisulphite-converted DNA samples ($Pml^{+/+}$ Ctrl, $Pml^{+/+}$ Dox, $Pml^{-/-}$ Ctrl, and $Pml^{-/-}$ Dox) were sequenced. Only methylation sites with a read number 10 were used for further study. MR of a methylation site was calculated as described in Materials and Methods. The alteration of methylation rate (AMR) of a site was calculated using the following formula: AMR = MR (Mock)/MR (Dox), where MR (Dox) and MR (Mock) are the MR of the sites with and without doxorubicin treatment,

respectively. Methylation sites with AMR > 1.5 and P < 0.05 were considered as significantly demethylated by doxorubicin. Smooth scatter plot of methylation sites demonstrated that most methylation sites (dark blue) of whole genome, CpG island, and none CpG island are located close to the red dash line (Fig. 6B). It means that the MR of most methylation sites was not notably altered by doxorubicin in $Pml^{+/+}$ (Fig. 6B) and $Pml^{-/-}$ (Supplementary Fig. S5A) MEF cells, which was consistent with the results of MS analyses (Supplementary Fig. S4D and S4E).

Next, we focused on the doxorubicin-promoted demethylation sites in WT cells (DPDMS-WT) to evaluate the impact of Pml on demethylation. Considering that lower MR (WT Mock) is inclined to disturb AMR value, we first analyzed the DPDMS-WTs with AMR > 1.5, P < 0.05, and MR (WT Mock) > 0.5. Because the methylation sites of the whole genome were formed by the methylation sites of CpG island and none CpG island, only the methylation sites of CpG island and none CpG island are shown. As shown in Fig. 6C, top, DPDMS-WTs with AMR > 1.5, P < 0.05, and MR (WT Mock) > 0.5 were far away from the red dash line, whereas most of the corresponding methylation sites were localized close to the red dash line in $Pml^{-/-}$ (Pml KO) cells (Fig. 6C, lower panel), which meant that Pml KO did abolish most of doxorubicin-promoted demethylation. Further analyses of DPDMS-WTs with MR (WT Mock) > 0.7 or MR (WT Mock) > 0.9 also argued that PML KO diminished doxorubicin-promoted demethylation (Supplementary Fig. S5B and S5C). Using AMR > 1.5 (demethylated), AMR < 0.5 (methylated) and 0.5 < AMR < 1.5 (not altered) as threshold, we then assessed the alteration of DPDMS-WTs described above in KO cells. As shown in Fig. 6D, about 95% of these corresponding DPDMS-WTs showed not alteration in KO cells.

To evaluate the impact of Pml on doxorubicin-promoted demethylation of particular genes, we compared the doxorubicin-promoted differentially methylated regions (DMR) of WT cells with DMR of KO cells. DMRs with MR (Dox)/MR (Mock) < 0.4 and P < 0.05 were taken as doxorubicin-promoted demethylation DMRs (DPD-DMRs). As expected, Pml KO resulted in notable alteration of DPD-DMRs (Fig. 6E). Twenty-one genes with DPD-DMRs located in ± 10 KB of TSS in WT cells are shown in Fig. 6F. Nineteen out of these twenty-one genes showing no difference [MR (Dox)/MR (Mock) > 0.9] in Pml KO cells were used for the further study. qRT-PCR of these genes indicated that doxorubicin showed the most notable ability to enhance Sim2 in WT cells, while Pml KO diminished the doxorubicin-promoted Sim2 expression (Fig. 6G). Further Western blotting confirmed that Pml KO decreased the doxorubicin-promoted Sim2 expression (Fig. 6H). And the recombinant adenovirus-mediated expression of PML in KO cells restored the ability of doxorubicin to enhance Sim2 (Fig. 6I and 6J).

To investigate the role of Tet2 and Pml in the demethylation and sequential transcription of Sim2, we carried out 5-hydroxymethylcytosine methylated DNA immunoprecipitation qPCR (hMEDIP-qPCR) analysis of Sim2 DMR. As shown in Fig. 6K, Sim2 DMR (Chr16:94095399–94095781) is located in the third exon of Sim2 and about 5 KB to downstream of Sim2 TSS. HMEDIP-qPCR of Sim2 DMR indicated that the doxorubicin-promoted 5hmC was decreased by the depletion of either Tet2 or Pml, but not additively by the codepletion of both genes (Fig. 6L). Further sodium bisulfite sequencing PCR of Sim2 DMR demonstrated that doxorubicin-promoted demethylation of Sim2 was diminished by

the depletion of either Tet2 or Pml, but not additively by the codepletion of both genes (Fig. 6M). Consistent with the observations of 5hmC and demethylation, the doxorubicin-induced expression of Sim2 was inhibited by the depletion of either Tet2 or Pml (Fig. 6N). Finally, the recombinant lentivirus-mediated expression of Sim2 was carried out to evaluate the physical role of Sim2 (Fig.6O). MTT analyses of the resultant cells indicated that enhanced expression of Sim2 impaired cell proliferation (Fig. 6P).

PML-TET2 regulates cell proliferation in response to doxorubicin

To investigate the effect of PML and TET2 on cell proliferation in response to chemotherapeutic agent, we overexpressed/knocked down PML and/or TET2 in multiple cell lines, and treated resultant cells with different doses of doxorubicin. A TET2 catalytic dead mutant (TET2 MUT) was used as negative control (Supplementary Fig. S5D and S5E). Unlike TET2 WT, TET2 MUT was not able to enhance 5hmC (Fig. 7A and 7B; Supplementary Fig. S5D and S5E). Enhanced expression of PML and/or TET2 WT increased the ability of doxorubicin to inhibit cell proliferation, whereas TET2 MUT showed no ability to enhance doxorubicin-promoted inhibition of cell proliferation (Fig. 7C). Interestingly, coexpression of PML and TET2 WT showed the most marked ability to sensitize HEK293 cells to doxorubicin (Fig.7C). Furthermore, siRNA- or shRNA-mediated knockdown of PML and/or TET2 resulted in poorer response to doxorubicin in MEF (Fig. 7D), HEK293 (Fig. 7E), SCC-15 (Fig. 7F), and SCC-25 cells (Fig. 7G). Comparing with knock down of PML, we did not detect additive ability of PML-TET2 codepletion to decrease response to doxorubicin (Fig. 7D-7G).

To investigate the role of PML and TET2 in response to doxorubicin *in vivo*, a xenograft mouse model was built. Briefly, SCC-15 cells stably expressing shScram (control scrambled shRNA), shPML, shTET2, or shPML/shTET2 were injected subcutaneously into the flank of mice. Then, these grouped tumor-bearing mice were treated with vehicle or doxorubicin. Consistent with the observation *in vitro*, knockdown of PML and/or TET2 resulted in poorer response to doxorubicin (Fig. 7H). To further evaluate the role of PML and TET2 *in vivo*, we examined the clinical relevance in HNSC patients. Using data set from The Cancer Genome Atlas (42), Kaplan-Meier plotter was built to analyze the overall survival of HNSC patients with different PML and TET2 levels. mRNA expression z-scores were calculated as described in cBioPortal (42). Default ±2 z-scores recommended by cBioPortal were used as threshold. Patients with PML or TET2 mRNA expression z-score > 2 were grouped into PML or TET2 high group (n = 52). The rest of the patients were grouped into PML and TET2 low group (n = 465). As shown in Fig. 7I, low expression of PML and TET2 was associated with poorer overall survival in HNSC patients.

Discussion

Aberrant DNA methylation leads to inappropriate transcriptional silencing and contributes to cancer progression. In response to therapies, failure to demethylate and to consequently reactivate these methylation-silenced tumor suppressors is a contributor to therapeutic resistance (2). One of the highly possible reasons for the failure to demethylate these methylated genes is the deregulation of TET pathway. However, the regulatory mechanism

of TETs in response to chemotherapeutic agents remains elusive. We found that multiple chemotherapeutic agents could enhance 5hmC through TET2. Further study indicated that PML physically bound to TET2 and recruited TET2 to PML-NBs in a PML C-terminal dependent way, and this binding between PML and TET2 could be disrupted by PML-RARA t(15;17) mutation. In response to doxorubicin, PML recruited TET2, regulated DNA modification, reactivated the methylation-silenced genes, and impaired cell proliferation, while knockout of PML abolished doxorubicin-promoted DNA modification. Additionally, PML and TET2 levels were positively correlated with improved overall survival in HSNC patients.

First, our study suggests that restoring demethylation pathways in certain cancer cells may increase their susceptibility to chemotherapy. Accumulating evidence indicate that the capacity of most cancers to resist chemotherapies is frequently connected to abnormalities of DNA methylation (2). One of the highly possible reasons for abnormal DNA methylation in cancer is the deregulation of TET pathway. This is supported by the observation that decreased TET and loss of 5hmC are seen in a wide variety of solid tumors (16, 17). Importantly, recent studies demonstrate that restoration of TET functions by genetic or pharmacological (ascorbate) methods itself could suppress cancer progression (43, 44). Our results suggest that activator of TETs (such as ascorbate) may act as an adjuvant to standard chemotherapy in future clinical trials. If the combination of chemotherapy and the activator of TETs shows acceptable tolerability in cancer patients, we expect that the combination should demonstrate synergistic effect. Furthermore, considering the function of PML and TET2 in tumors, we propose that measuring the levels of PML and/or TET2 may help to predict the interactions between chemotherapy and the activator of TETs.

Second, the potential pathological significance of PML and TET2 interaction is at least side supported by the observation that PML interacts with TET2, depending on the PML C-terminal, which is not included in PML-RARA fusion protein. PML-RARA, resulting from the displacement of PML C-terminal with RARA through t(15;17), is proven to promote APL (45). Chemotherapy using As_2O_3 and RA induces clinical remission of APL through degradation of PML-RARA and reorganization of PML-NBs (46, 47). Consistent with this, we found that As_2O_3 and RA degraded PML-RARA and enhanced 5hmC, the intermediate of DNA demethylation. Interestingly, DNMT3A-mediated DNA methylation is essential for PML-RARA to initiate APL (22). Considering the critical roles of 5hmC in DNA demethylation and sequential transcription activation, our study suggests that PML-RARA t(15;17) mutation potentially disrupts the transcription-activating function of PML and TET2. More study is still required to investigate the role of TET2 in the initiation and therapy of APL.

Thirdly, our study also suggests that PML and TET2 interaction may be involved in other pathways. PML is well known to recruit numerous transcription factors to PML-NB to regulate transcription in response to a wide variety of stimuli (such as chemotherapy, hypoxia, and virus infection) (23). PML-NBs are frequently localized to particularly gene-rich and transcriptional active regions of chromatin (48). Although it is arguable whether PML itself is a transcription factor, previous studies have demonstrated that PML plays critical roles in stimulus-promoted transcription (20, 23). In this study, we showed that

chemotherapeutic agents promote PML-NB, delocalize TET2, enhance 5hmC, and result in DNA demethylation (Fig. 7J). Interestingly, previous studies have demonstrated that PML and 5hmC share the same binding partners such as p53 (20, 49), which suggests that PML might promote 5hmC and recruit 5hmC reader transcription factors to control transcription. Hence, we speculate that PML may also facilitate the association of TET2 and transcription factors (Fig. 7J). Considering the number of PML-modulating stimuli (such as hypoxia and inflammation) (23, 50) and PML-modulated transcription factors (23), PML-TET2 might be involved in multiple pathways.

However, several limitations should be noted. Firstly, although meta-analysis indicated that PML (PML-RARA) and TET2 were mutated mutually exclusively in AML, this exclusive distribution should not be taken as proof (at least not a strong proof) to support that PML and TET2 function in the same pathway. This is due to the origin and differentiation state difference between APL (PML-RARA) and other AMLs. Secondly, we concentrated on only TET-dependent DNA demethylation in response to chemotherapies. There might be some TET-independent demethylation pathways in response to chemotherapies. Thirdly, we focused our study on only several cell lines. Considering that DNA methylation might show different patterns in a cancer-type-specific and even cell-type-specific manner, we only carried out whole genomic bisulfite sequencing of MEF cells. Despite these limitations, this study does indicate that PML and TET2 regulate DNA modification in response to chemotherapeutic agents.

Collectively, we describe that PML recruits TET2 to regulate DNA modification and cell proliferation in response to chemotherapeutic agents, which might potentially contribute to the improvement of cancer therapies.

Supplementary Material

Refer to Web version on PubMed Central for supplementary material.

Acknowledgments

References

1. Shen H, Laird PW. Interplay between the cancer genome and epigenome. Cell 2013;153(1):38–55. [PubMed: 23540689]

2. Rodriguez-Paredes M, Esteller M. Cancer epigenetics reaches mainstream oncology. Nature medicine 2011;17(3):330–9.

3. Kohli RM, Zhang Y. TET enzymes, TDG and the dynamics of DNA demethylation. Nature 2013;502(7472):472–9. [PubMed: 24153300]

4. Alderton GK. Leukaemia and lymphoma: The expansive reach of TET2. Nature reviews 2011;11(8): 535.

5. Moran-Crusio K, Reavie L, Shih A, et al. Tet2 loss leads to increased hematopoietic stem cell self-renewal and myeloid transformation. Cancer Cell 2011;20(1):11–24. [PubMed: 21723200]

6. Ko M, Bandukwala HS, An J, et al. Ten-Eleven-Translocation 2 (TET2) negatively regulates homeostasis and differentiation of hematopoietic stem cells in mice. Proceedings of the National Academy of Sciences of the United States of America 2011;108(35):14566–71. [PubMed: 21873190]

7. Ko M, Huang Y, Jankowska AM, et al. Impaired hydroxylation of 5-methylcytosine in myeloid cancers with mutant TET2. Nature 2010;468(7325):839–43. [PubMed: 21057493]

8. Delhommeau F, Dupont S, Della Valle V, et al. Mutation in TET2 in myeloid cancers. The New England journal of medicine 2009;360(22):2289–301. [PubMed: 19474426]

9. Kandoth C, McLellan MD, Vandin F, et al. Mutational landscape and significance across 12 major cancer types. Nature 2013;502(7471):333–9. [PubMed: 24132290]

10. Metzeler KH, Maharry K, Radmacher MD, et al. TET2 mutations improve the new European LeukemiaNet risk classification of acute myeloid leukemia: a Cancer and Leukemia Group B study. J Clin Oncol 2011;29(10):1373–81. [PubMed: 21343549]

11. Abdel-Wahab O, Mullally A, Hedvat C, et al. Genetic characterization of TET1, TET2, and TET3 alterations in myeloid malignancies. Blood 2009;114(1):144–7. [PubMed: 19420352]

12. Figueroa ME, Abdel-Wahab O, Lu C, et al. Leukemic IDH1 and IDH2 mutations result in a hypermethylation phenotype, disrupt TET2 function, and impair hematopoietic differentiation. Cancer Cell 2010;18(6):553–67. [PubMed: 21130701]

13. Xu W, Yang H, Liu Y, et al. Oncometabolite 2-hydroxyglutarate is a competitive inhibitor of alpha-ketoglutarate-dependent dioxygenases. Cancer Cell 2011;19(1):17–30. [PubMed: 21251613]

14. Rampal R, Alkalin A, Madzo J, et al. DNA hydroxymethylation profiling reveals that WT1 mutations result in loss of TET2 function in acute myeloid leukemia. Cell Rep 2014;9(5):1841–55. [PubMed: 25482556]

15. Wang Y, Xiao M, Chen X, et al. WT1 recruits TET2 to regulate its target gene expression and suppress leukemia cell proliferation. Molecular cell 2015;57(4):662–73. [PubMed: 25601757]

16. Lian CG, Xu Y, Ceol C, et al. Loss of 5-hydroxymethylcytosine is an epigenetic hallmark of melanoma. Cell 2012;150(6):1135–46. [PubMed: 22980977]

17. Yang H, Liu Y, Bai F, et al. Tumor development is associated with decrease of TET gene expression and 5-methylcytosine hydroxylation. Oncogene 2013;32(5):663–9. [PubMed: 22391558]

18. Song SJ, Poliseno L, Song MS, et al. MicroRNA-antagonism regulates breast cancer stemness and metastasis via TET-family-dependent chromatin remodeling. Cell 2013;154(2):311–24. [PubMed: 23830207]

19. Zeisig BB, Kulasekararaj AG, Mufti GJ, So CW. SnapShot: Acute myeloid leukemia. Cancer Cell 2012;22(5):698–e1. [PubMed: 23153541]

20. Bernardi R, Pandolfi PP. Structure, dynamics and functions of promyelocytic leukaemia nuclear bodies. Nat Rev Mol Cell Biol 2007;8(12):1006–16. [PubMed: 17928811]

21. Di Croce L, Raker VA, Corsaro M, et al. Methyltransferase recruitment and DNA hypermethylation of target promoters by an oncogenic transcription factor. Science 2002;295(5557):1079–82. [PubMed: 11834837]

22. Cole CB, Verdoni AM, Ketkar S, et al. PML-RARA requires DNA methyltransferase 3A to initiate acute promyelocytic leukemia. The Journal of clinical investigation 2016;126(1):85–98. [PubMed: 26595813]

23. Zhong S, Salomoni P, Pandolfi PP. The transcriptional role of PML and the nuclear body. Nat Cell Biol 2000;2(5):E85–90. [PubMed: 10806494]

24. Yang Q, Deng X, Lu B, et al. Pharmacological inhibition of BMK1 suppresses tumor growth through promyelocytic leukemia protein. Cancer Cell 2010;18(3):258–67. [PubMed: 20832753]

25. Qin X, Zheng C, Yates JR, 3rd, Liao L. Quantitative phosphoproteomic profiling of PINK1-deficient cells identifies phosphorylation changes in nuclear proteins. Molecular bioSystems 2014;10(7):1719–29. [PubMed: 24626860]

26. Chen RQ, Yang QK, Lu BW, et al. CDC25B mediates rapamycin-induced oncogenic responses in cancer cells. Cancer Res 2009;69(6):2663–8. [PubMed: 19276368]

27. Yang Q, Liao L, Deng X, et al. BMK1 is involved in the regulation of p53 through disrupting the PML-MDM2 interaction. Oncogene 2013;32(26):3156–64. [PubMed: 22869143]

28. Xu Q, Wang K, Wang L, et al. IDH1/2 Mutants Inhibit TET-Promoted Oxidation of RNA 5mC to 5hmC. PLoS One 2016;11(8):e0161261. [PubMed: 27548812]

29. Chen Q, Chen Y, Bian C, Fujiki R, Yu X. TET2 promotes histone O-GlcNAcylation during gene transcription. Nature 2013;493(7433):561–4. [PubMed: 23222540]

30. Ha K, Lee GE, Palii SS, et al. Rapid and transient recruitment of DNMT1 to DNA double-strand breaks is mediated by its interaction with multiple components of the DNA damage response machinery. Human molecular genetics 2011;20(1):126–40. [PubMed: 20940144]

31. Uy GL, Lane AA, Welch JS, Grieselhuber NR, Payton JE, Ley TJ. A protease-resistant PML-RAR{alpha} has increased leukemogenic potential in a murine model of acute promyelocytic leukemia. Blood 2010;116(18):3604–10. [PubMed: 20647568]

32. Song C, Wang L, Xu Q, et al. Targeting BMK1 Impairs the Drug Resistance to Combined Inhibition of BRAF and MEK1/2 in Melanoma. Sci Rep 2017;7:46244. [PubMed: 28387310]

33. Jackman J, O'Connor PM. Methods for synchronizing cells at specific stages of the cell cycle. Curr Protoc Cell Biol 2001;Chapter 8:Unit 8 3.

34. Guo JU, Su Y, Zhong C, Ming GL, Song H. Hydroxylation of 5-methylcytosine by TET1 promotes active DNA demethylation in the adult brain. Cell 2011;145(3):423–34. [PubMed: 21496894]

35. Wu H, D'Alessio AC, Ito S, et al. Genome-wide analysis of 5-hydroxymethylcytosine distribution reveals its dual function in transcriptional regulation in mouse embryonic stem cells. Genes Dev 2011;25(7):679–84. [PubMed: 21460036]

36. Thienpont B, Steinbacher J, Zhao H, et al. Tumour hypoxia causes DNA hypermethylation by reducing TET activity. Nature 2016;537(7618):63–8. [PubMed: 27533040]

37. Nisole S, Maroui MA, Mascle XH, Aubry M, Chelbi-Alix MK. Differential Roles of PML Isoforms. Frontiers in oncology 2013;3:125. [PubMed: 23734343]

38. TCGA. Genomic and epigenomic landscapes of adult de novo acute myeloid leukemia. The New England journal of medicine 2013;368(22):2059–74. [PubMed: 23634996]

39. Liang DC, Liu HC, Yang CP, et al. Cooperating gene mutations in childhood acute myeloid leukemia with special reference on mutations of ASXL1, TET2, IDH1, IDH2, and DNMT3A. Blood 2013;121(15):2988–95. [PubMed: 23365461]

40. Welch JS, Ley TJ, Link DC, et al. The origin and evolution of mutations in acute myeloid leukemia. Cell 2012;150(2):264–78. [PubMed: 22817890]

41. Papaemmanuil E, Gerstung M, Bullinger L, et al. Genomic Classification and Prognosis in Acute Myeloid Leukemia. The New England journal of medicine 2016;374(23):2209–21. [PubMed: 27276561]

42. Cerami E, Gao J, Dogrusoz U, et al. The cBio cancer genomics portal: an open platform for exploring multidimensional cancer genomics data. Cancer discovery 2012;2(5):401–4. [PubMed: 22588877]

43. Agathocleous M, Meacham CE, Burgess RJ, et al. Ascorbate regulates haematopoietic stem cell function and leukaemogenesis. Nature 2017;549(7673):476–81. [PubMed: 28825709]

44. Cimmino L, Dolgalev I, Wang Y, et al. Restoration of TET2 Function Blocks Aberrant Self-Renewal and Leukemia Progression. Cell 2017;170(6):1079–95 e20. [PubMed: 28823558]

45. Mu ZM, Chin KV, Liu JH, Lozano G, Chang KS. PML, a growth suppressor disrupted in acute promyelocytic leukemia. Molecular and cellular biology 1994;14(10):6858–67. [PubMed: 7935403]

46. Dyck JA, Maul GG, Miller WH, Jr., Chen JD, Kakizuka A, Evans RM. A novel macromolecular structure is a target of the promyelocyte-retinoic acid receptor oncoprotein. Cell 1994;76(2):333–43. [PubMed: 8293467]

47. Weis K, Rambaud S, Lavau C, et al. Retinoic acid regulates aberrant nuclear localization of PML-RAR alpha in acute promyelocytic leukemia cells. Cell 1994;76(2):345–56. [PubMed: 8293468]

48. Sun Y, Durrin LK, Krontiris TG. Specific interaction of PML bodies with the TP53 locus in Jurkat interphase nuclei. Genomics 2003;82(2):250–2. [PubMed: 12837275]

49. Spruijt CG, Gnerlich F, Smits AH, et al. Dynamic readers for 5-(hydroxy)methylcytosine and its oxidized derivatives. Cell 2013;152(5):1146–59. [PubMed: 23434322]

50. Wang ZG, Ruggero D, Ronchetti S, et al. PML is essential for multiple apoptotic pathways. Nature genetics 1998;20(3):266–72. [PubMed: 9806545]

Significance:

Promyeloctic leukemia protein recruits TET2, regulating DNA modification and cell proliferation in response to chemotherapeutic agents.
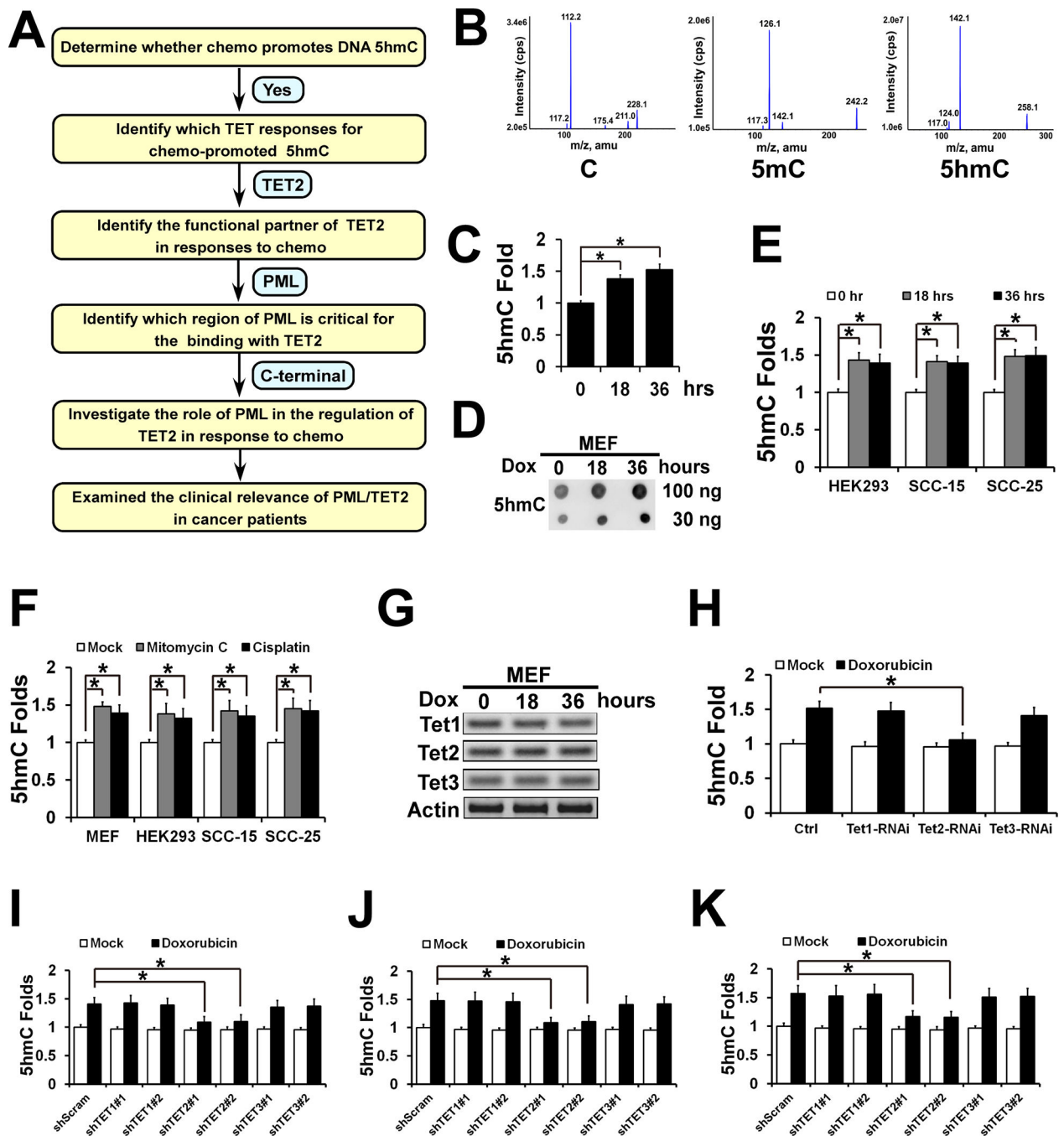
Figure 1.

TET2 promotes DNA 5hmC modification in response to chemotherapeutic agents. **A,** Schemamtic of this study. **B,** Base ion mass transitions for LC-MS/MS analysis of dC, 5mdC and 5hmdC. The nucleosides were quantified using the nucleoside to base ion mass transitions of 228 to 112 (C), 242 to 126 (5mC) and 258 to 142 (5hmC). **C,** LC-MS/MS analysis of 5hmC levels of MEF cells treated with 500 nM doxorubicin. The DNA 5hmC (5hmC/C) and 5mC (5mC/C) levels (n = 3 and ± SEM) were assessed by MS unless specifically noted. *P* values of MS analyses were calculated using Student's *t*-test and *p*

value < 0.05 was considered as significant (*).The 5hmC of the cells treated with doxorubicin for 0 hr was considered as 1. **D,** 5hmC dot blot assay of MEF cells treated with doxorubicin for 0, 18 or 36 hrs. **E,** LC-MS/MS analysis of 5hmC levels of HEK293, SCC-15 and SCC-25 cells treated with 500 nM doxorubicin. **F,** The 5hmC levels of MEF, HEK293, SCC-15 and SCC-25 cells treated with mitomycin C (6 μM) or cisplatin (2 μM) for 36 hrs. **G,** Western blotting showing the protein levels of Tet1, Tet2 and Tte3 in MEF cells treated with doxorubicin. **H,** The 5hmC levels of MEF cells treated with siRNAs and/or doxorubicin as noted. MEF cells were tranfected with smart pool siRNAs against control (nontargeting), Tet1, Tet2 or Tet3. After 24 hrs, the cells were treated with doxorubicin for 30 hrs. **I, J** and **K,** The 5hmC level of stable TET knockdown HEK293 (**I**), SCC-15 (**J**) and SCC-25 (**K**) cells treated with mock or doxorubicin for 36 hrs.
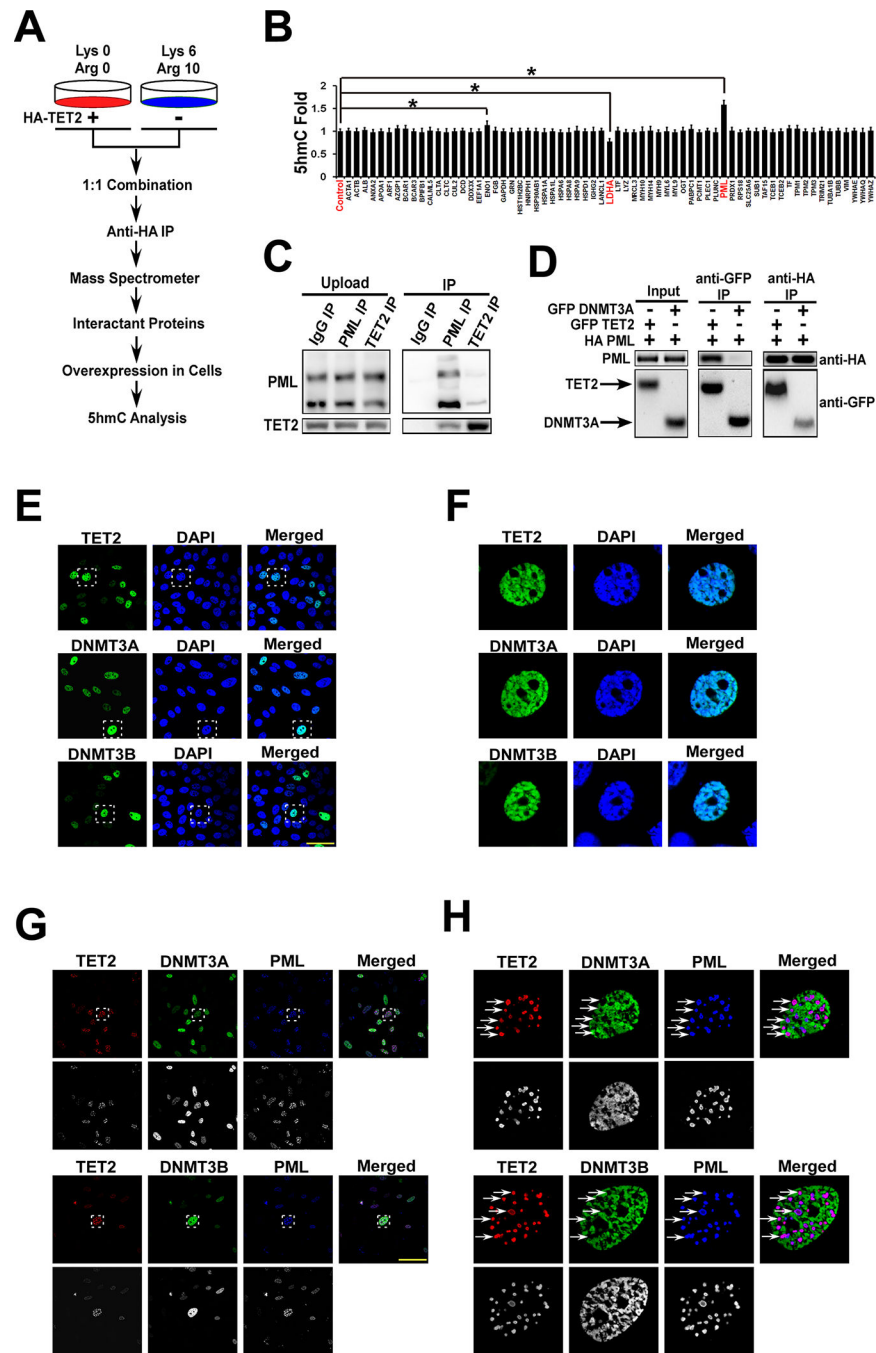
Figure 2.
PML physically binds to TET2 and recruits TET2 to PML nuclear bodies. **A,** Schemamtic showing SILAC-labeling and mass spectrometry analysis of anti-TET2 co-IP. **B,** The 5mC levels (5mC/C) of HEK293 cells transfected with the plasmids encoding 65 potential functional partners of TET2. The pCDH lentivector was used as control and the 5hmC level of pCDH-transfected HEK293 was taken as 1. **C,** Co-IP analysis of endogenous TET2 and PML in HEK293 cells. **D,** Co-IP analysis of EGFP-tagged TET2 and HA-tagged PML. pEGFP-DNMT3A, pEGFP-TET2 or HA-PML (IV) were transfected in HEK293 cells. Then

GFP-DNMT3A, GFP-TET2 and HA-PML were immunoprecipitated as noted. **E,** Fluorescent microscopy images of U2OS cells transfected with expression vectors containing pEGFP-TET2, pEGFP-DNMT3A or pEGFP-DNMT3B. Scale bar = 50 μm. **F,** The enlarged fluorescent microscopy images of the white rectangles in (**E**). **G,** Fluorescent microscopy images of U2OS cells transfected with HA-PML, pCI-Neo Flag-TET2, pEGFP-DNMT3A or pEGFP-DNMT3B. These cells were stained with anti-Flag (red, first-column panels) and anti-PML (blue, third-column panels) antibodies. Scale bar = 50 μm. **H,** The enlarged fluorescent microscopy images of the white rectangles in **G**. White arrows indicate that only Flag-TET2 is colocalized with PML-NBs.
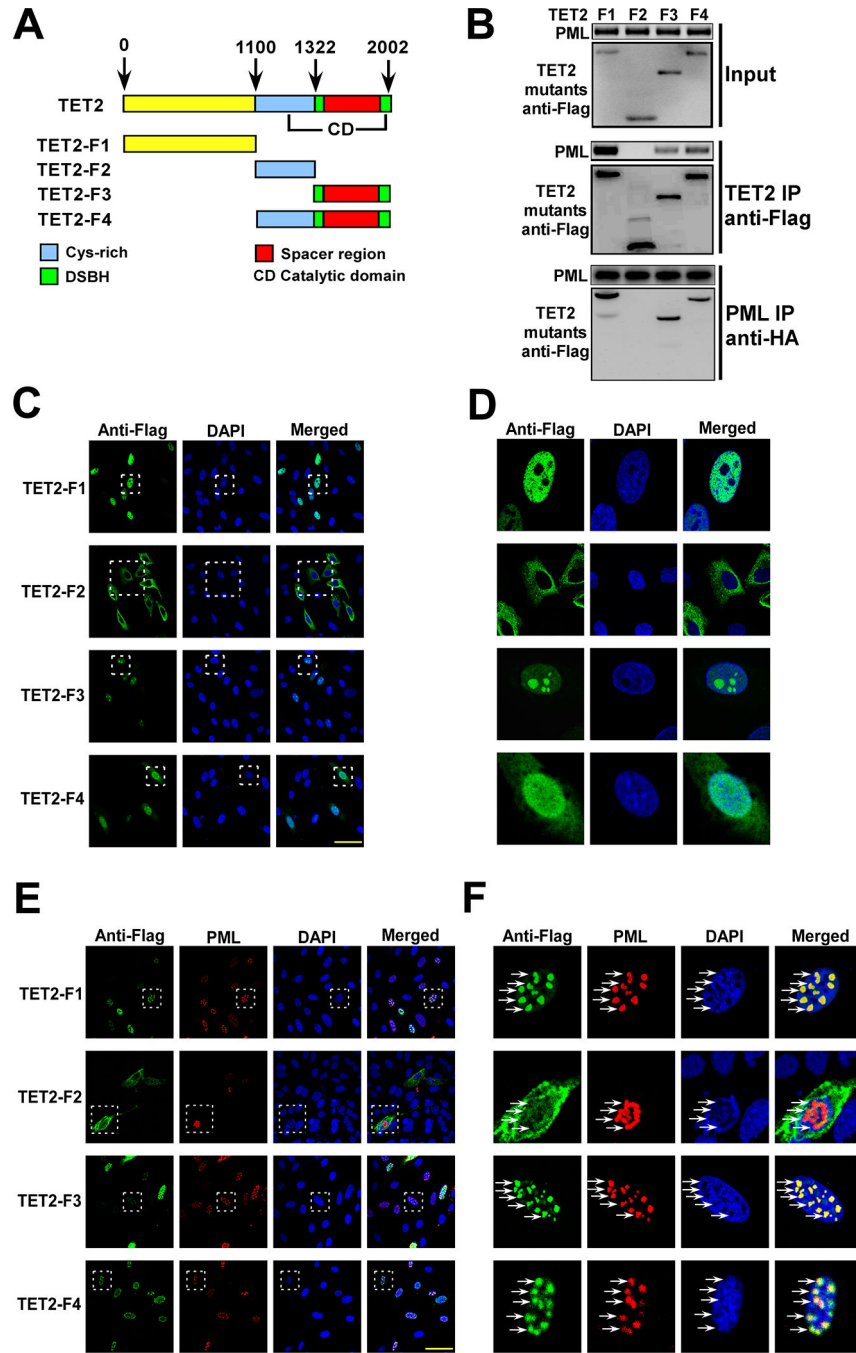
Figure 3.
The regions of TET2 to interact with PML. **A,** Schematic showing TET2-deletion mutants. **B,** Co-IP analysis of PML and TET2-deletion mutants. pS-Flag-SBP TET2-deletion mutants (F1-F4) or HA-PML were transfected into HEK293 cells. Then Flag tagged TET2-deletion mutants and HA-PML were immunoprecipitated. **C,** Fluorescent microscopy images of U2OS cells transfected with pS-Flag-SBP TET2-deletion mutants (F1-F4). Scale bar = 50 μm. **D,** The enlarged fluorescent microscopy images of the white rectangles in (**C**). **E,** Fluorescent microscopy images of U2OS cells transfected with pS-Flag-SBP TET2-deletion

mutants (F1-F4) and HA-PML. Scale bar = 50 μm. **F,** The enlarged fluorescent microscopy images of the white rectangles in (**E**). White arrows indicate the colocalization between TET2-deletion mutants and PML.
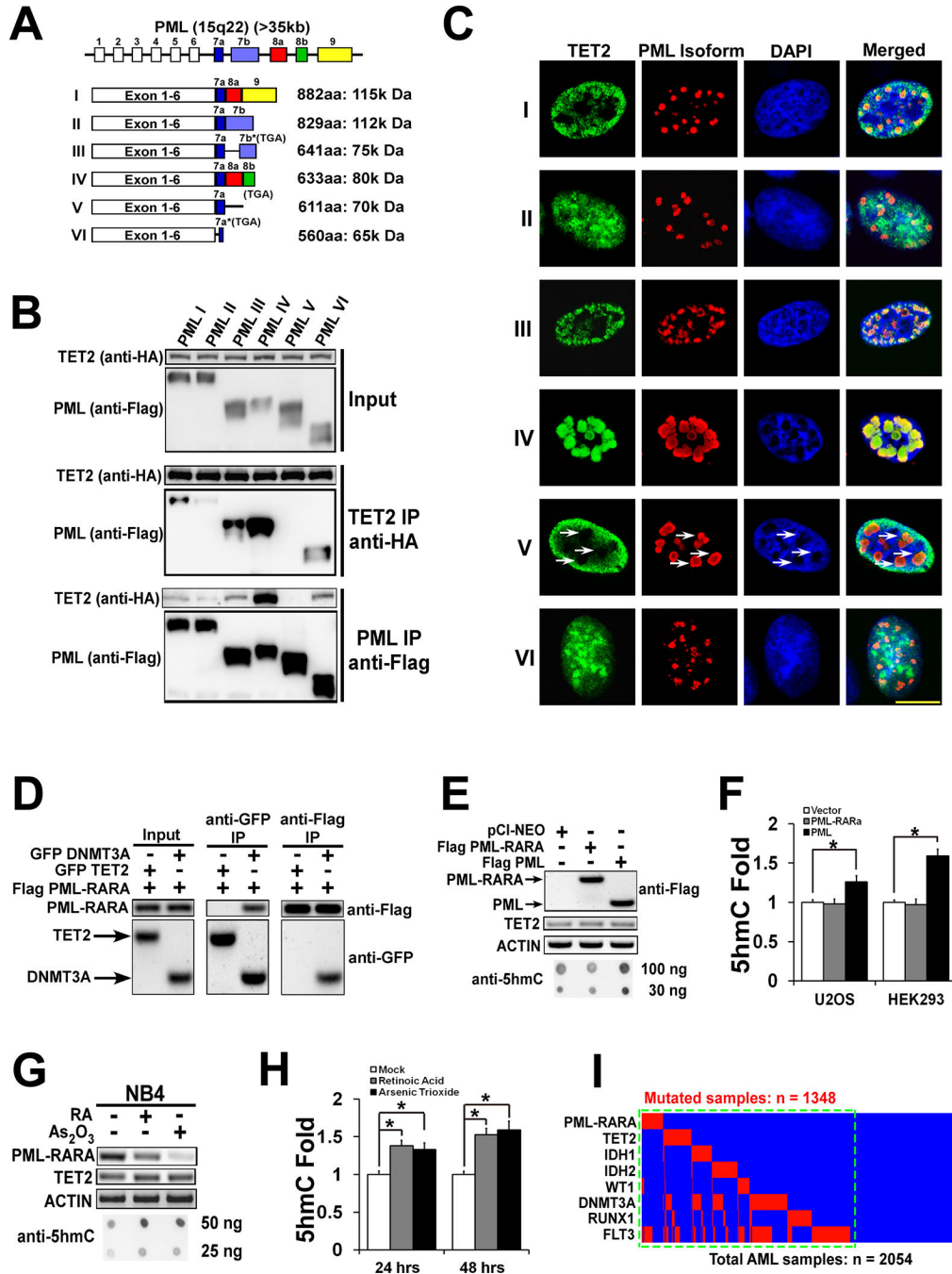
Figure 4.
PML-RARA t(15;17) mutation disrupts the ability of PML to bind TET2. **A,** Schematic showing primary structure of PML isoform I–VI. **B,** Co-IP analysis of TET2 and PML isoforms. pCI-Neo HA-TET2 and pCI-Neo Flag-PML isoforms (PML I-VI) were transfected into HEK293 cells. Then TET2 and PML I-VI were immunoprecipitated using anti-Flag and anti-HA antibodies. **C,** Fluorescent microscopy images of U2OS cells transfected with pCI-Neo HA-TET2 and pCI-Neo Flag-PML I-VI isoforms. These cells were stained with anti-HA and anti-PML antibodies. White arrows indicate the PML V

shows no colocalizaiotn with TET2. Scale bar = 10 μm. **D,** Co-IP analysis of DNMT3A, TET2 and PML-RARA. HEK293 cells were transfected with pEGFP-DNMT3A, pEGFP-TET2 and pCI-Neo Flag-PML-RARA. Then GFP-DNMT3A, GFP-TET2 and Flag-PML-RARA were immunoprecipitated as noted. **E,** The 5hmC dot blot analysis of HEK293 transfected with pCI-NEO, pCI-NEO-Flag PML-RARA or pCI-NEO-Flag PML IV for 36 hrs. **F,** The 5hmC levels of HEK293 and U2OS transfected with pCI-NEO, pCI-NEO-Flag PML-RARA or pCI-NEO-Flag PML IV for 36 hrs. **G,** The 5hmC dot blot analysis of NB4 cells treated with 5 μM RA or 1 μM arsenic acid (As_2O_3) for 36 hrs. **H,** The 5hmC levels of NB4 cells treated with RA or As_2O_3 for 24 or 48 hrs. **I,** Somatic mutations (containing point mutation, internal tandem duplication, chromosome translocation mutation and gene deletion) in PML-RARA, TET2, IDH1, IDH 2, WT1, DNMT3A, RUNX1 and FLT3 were identified in 2054 AML cases, which were from four studies (38–41). 1348 out of 2054 cases carried at least one mutation. Odd Ratio was calculated using the formula: Odd Ratio = (A * D)/(B * C), where A = number of cases altered in both genes; B = number of cases altered in G1 but not G2; C = number of cases altered in G2 but not G1; and D = number of cases altered in neither gene. Fisher's exact test was used for the calculation of *p* value.
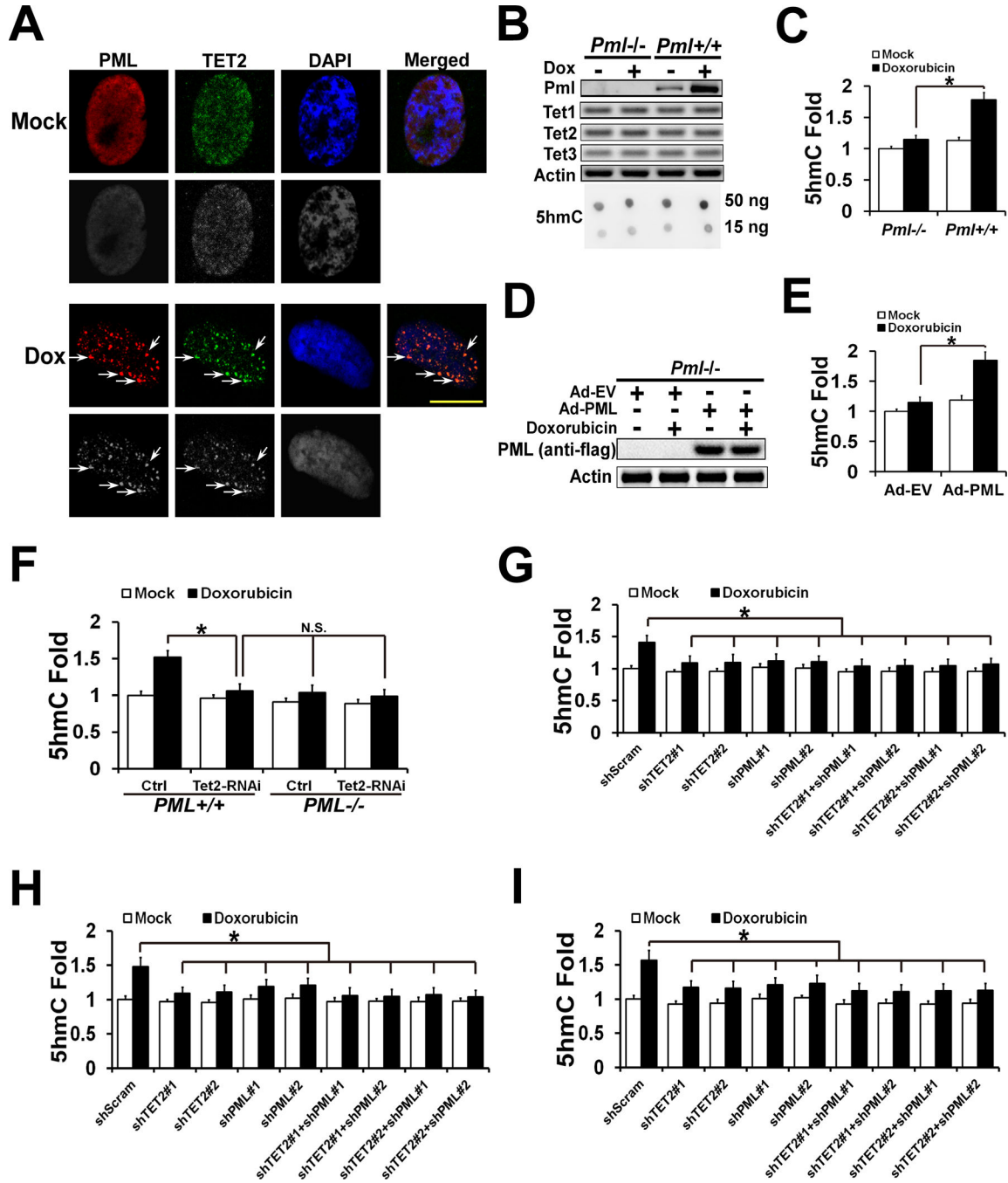
Figure 5.
PML recruits TET2 to regulate DNA 5hmC modification in response to chemotherapies. **A,**
Representative fluorescent microscopy images of SCC-15 cells treated with doxorubicin for
30 hrs. White arrows indicate the doxorubicin promoted colocalization between PML and
TET2. Scale bar = 10 μm. **B,** $Pml^{+/+}$ and $Pml^{-/-}$ MEF cells were treated with doxorubicin
for 36 hrs. Resultant cell lysates and DNA samples were analyzed by western blot and MS,
respectively. **C,** MS analysis of the 5hmC levels of the cells described in (**B**). **D,** $Pml^{-/-}$
MEF cells were infected with adenovirus encoding empty vector (Ad-EV) or Flag tagged

PML (Ad-PML) for 24 hrs. Then cells were treated with doxorubicin for 24 hrs. **E,** The 5hmC levels of the cells described in (**D**). **F,** The 5hmC levels of $Pml^{+/+}$ and $Pml^{-/-}$ MEF cells treated with Tet2 siRNAs and/or doxorubicin. $Pml^{+/+}$ and $Pml^{-/-}$ MEF cells were tranfected with control (nontargeting) or Tet2 siRNAs. After 24 hrs, the cells were treated with doxorubicin for 30 hrs. **G, H,** and **I,** The 5hmC level of stable TET2, PML, and TET2+PML knockdown HEK293 (**G**), SCC-15 (**H**) and SCC-25 (**I**) cells treated with doxorubicin for 36 hrs. These stable cell lines were generated as described in Materials and Methods.
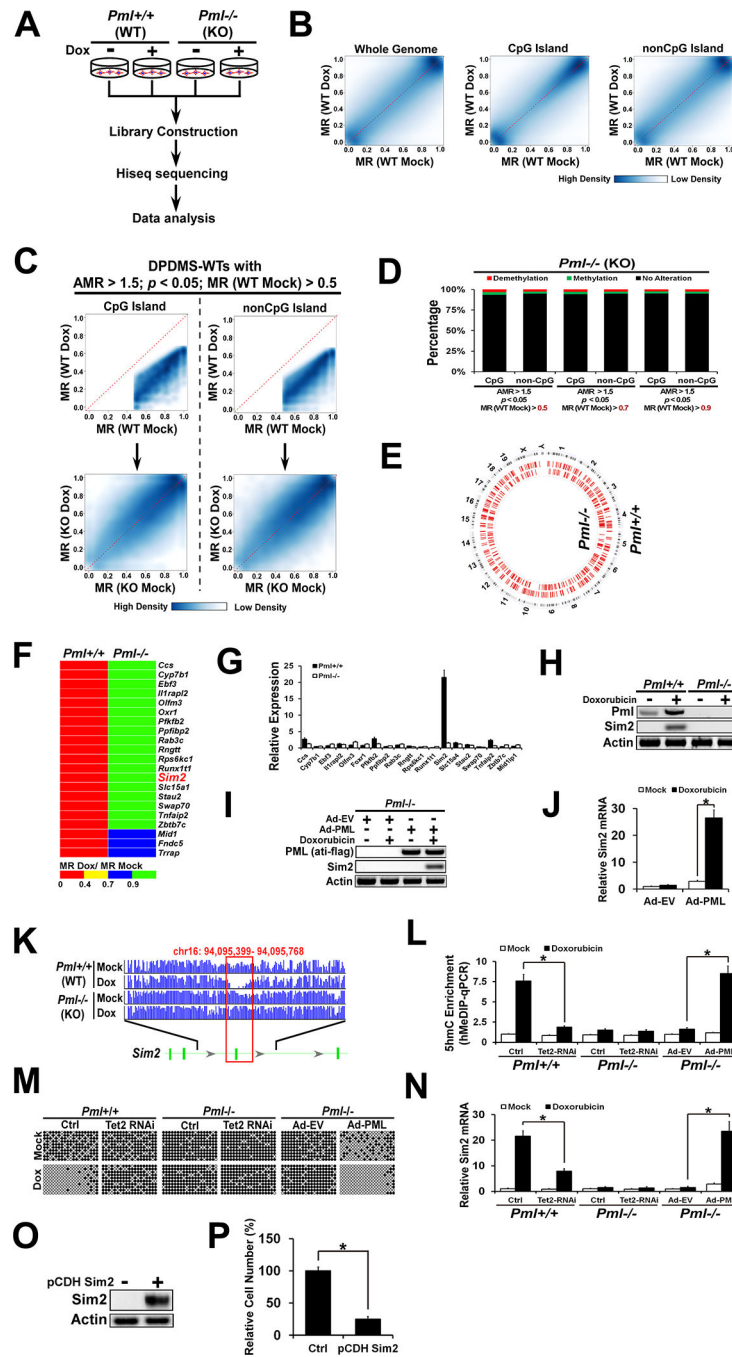
Figure 6.

Knockout of PML diminishes doxorubicin-promoted demethylation. **A,** Schematic showing whole genomic bisulfite sequencing of *Pml*^{+/+} and *Pml*^{−/−} MEF cells treated with doxorubicin for 30 hrs. **B,** Smooth scatter plot showing the methylation rate correlation between Mock (control, X-axis) and Dox (doxorubicin treatment, Y-axis) in *Pml*^{+/+} WT MEF cells. The numbers (ranging from 0 to 1) in both axes represent MR. The red dash line represents AMR = 1 (no MR alteration) and the colors from dark blue to white represent the relative density of methylation sites. **C,** Smooth scatter plot showing DPDMS-WT

methylation status in $Pml^{-/-}$ KO cells. AMR = MR (WT Mock)/ MR (WT Dox) > 1.5, MR (Mock) > 0.5 and p value < 0.05 were taken as the thresholds of DPDMS-WTs in $Pml^{+/+}$ WT cells. The resultant DPDMS-WTs (upper panel) were used to build the smooth scatter plot to show the correlation between MR (KO Mock) and MR (KO Dox) in $Pml^{-/-}$ KO cells (lower panel). **D,** Percentages of different DPDMS-WT methylation status in $Pml^{-/-}$ KO cells. Red: DPDMSs with AMR (KO) > 1.5 and p value <0.05 in Pml KO cells; green: DPDMSs with AMR (KO) < 0.5 and p value < 0.05 in KO cells; black: no significant altered sites in KO cells. **E,** Circular plot showing genome-wide doxorubicin-promoted demethylation DMRs in $Pml^{+/+}$ and $Pml^{-/-}$ MEF cells. Red scales represent DPD-DMRs. **F,** Heat map of 21 genes with DPD-DMRs in Pml WT and KO cells. **G,** QRT-PCR analysis of the gene expression in $Pml^{+/+}$ and $Pml^{-/-}$ MEF cells treated with doxorubicin for 36 hrs. **H,** Western blotting showing Pml and Sim2 in $Pml^{+/+}$ and $Pml^{-/-}$ MEF cells treated with doxorubicin for 36 hrs. **I,** $Pml^{-/-}$ MEF cells were infected with adenovirus encoding Ad-EV (empty vector) or Ad-PML (Flag-PML) for 24 hrs. The resultant cells were treated with doxorubicin for 24 hrs. **J,** QRT-PCR analysis of Sim2 expression in the cells described in (**I**). **K,** Genome browser view showing demethylation regions in Sim2 gene. Only methylation sites with the number of reads 10 were used. The scales represent the methylation rates ranging from 0 to 1. **L,** The 5hmC levels of Sim2 DMR in $Pml^{+/+}$ and $Pml^{-/-}$ MEF cells treated with doxorubicin. $Pml^{+/+}$ and $Pml^{-/-}$ MEF cells were tranfected with siRNAs as noted. After 30 hrs, the cells were treated with doxorubicin for 12 hrs. Then 5hmC levels of Sim2 DMR were determined by hMEDIP-qPCR. **M,** The 5mC levels of Sim2 DMR in $Pml^{+/+}$ and $Pml^{-/-}$ MEF cells treated with doxorubicin. $Pml^{+/+}$ and $Pml^{-/-}$ MEF cells tranfected with siRNAs as noted. After 30 hrs, the cells were treated with doxorubicin for 24 hrs. Sodium bisulfite sequencing PCR of Sim2 was carried out to assess the 5mC level. Open circles are unmethylated CpGs and black filled circles are methylated CpGs. **N,** QRT-PCR analysis of Sim2 mRNA expression in the cells described in (**M**). **O,** MEF cells were infected with lentivirus encoding pCDH (empty vector) or pCDH Sim2 (Flag-Sim2) for 48 hrs. **P,** Relative cell number of MEF cells infected with lentivirus encoding pCDH (empty vector) or pCDH Sim2 (Flag-Sim2) for 60 hrs. MTT analysis was carried out to assess the cell number.
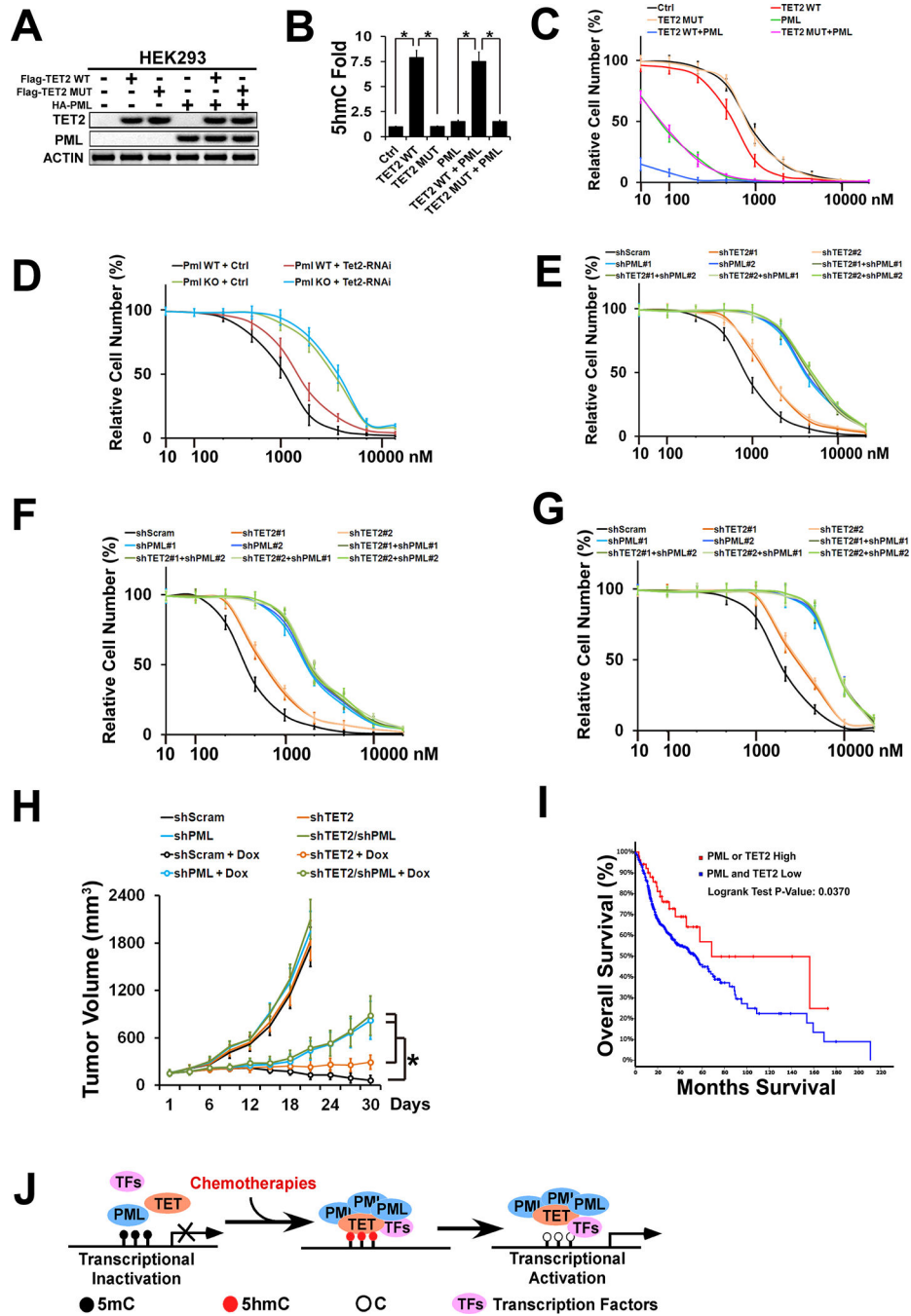
Figure 7.
PML-TET2 regulates cell proliferation in response to chemotherapy. **A,** Western blotting showing Flag-TET2 and HA-PML in HEK293 cells were transfected with HA-PML, pCDNA3B Flag-TET2 WT or pCDNA3B Flag-TET2 MUT for 48 hrs. **B,** The 5mC levels of the cells described in (**A**). **C,** HEK293 cells transfected with HA-PML, pCDNA3B Flag-TET2 WT or pCDNA3B Flag-TET2 MUT for 24 hrs. Then the cells were treated with 0, 10, 100, 250, 500, 1000, 2500, 5000, 10000 or 25000 nM of doxorubicin for 48 hrs. The cell number of the cells without doxorubicin treatment was taken as 100%. **D,** Relative cell

number of *Pml*^{+/+} and *Pml*^{−/−} cells treated with Tet2 siRNAs and/or doxorubicin. *Pml*^{+/+} and *Pml*^{−/−} MEF cells were tranfected with control (nontargeting) or Tet2 siRNAs for 24 hrs. Then resultant cells were treated with doxorubicin for 48 hrs. **E, F,** and **G,** Relative cell number of stable TET2 and/or PML knockdown HEK293 (**E**), SCC-15 (**F**) and SCC-25 (**G**) cells treated with doxorubicin. The stable cells were treated with doxorubicin for 60 hrs. **H,** Mouse SCC-15 stable cell xenograft models treated with doxorubicin. n = 8 groups; n = 6 mice/group; ± SEM. **I,** Kaplan-Meier Plotter of the overall survival of head and necks patients with different PML-TET2 levels. More details about HNSC patients are described in Supplementary Table S3. **J,** Schematic showing PML-TET2-promoted DNA demethylation in response to chemotherapy.